34. Elferink RO, Groen AK. Genetic defects in hepatobiliary transport. Biochim Biophys Acta 2002;1586:129–145.
35. Figge A, Lammert F, Paigen B, et al. Hepatic overexpression of murine Abcb11 increases hepatobiliary lipid secretion and reduces hepatic steatosis. J Biol Chem 2004;279:2790–2799.
36. Smit JJ, Schinkel AH, Oude Elferink RP, et al. Homozygous disruption of the murine mdr2 P-glycoprotein gene leads to a complete absence of phospholipid from bile and to liver disease. Cell 1993;75:451–462.
37. Wiersma H, Gatti A, Nijstad N, et al. Scavenger receptor class B type I mediates biliary cholesterol secretion independent of ATP-binding cassette transporter g5/g8 in mice. Hepatology 2009;50:1263–1272.
38. Plosch T, van der Veen JN, Havinga R, et al. Abcg5/Abcg8-independent pathways contribute to hepatobiliary cholesterol secretion in mice. Am J Physiol Gastrointest Liver Physiol 2006;291:G414–G423.
39. Groen A, Kunne C, Jongsma G, et al. Abcg5/8 independent biliary cholesterol excretion in Atp8b1-deficient mice. Gastroenterology 2008;134:2091–2100.
40. Groen AK, Elferink RP, Tager JM. Control analysis of biliary lipid secretion. J Theor Biol 1996;182:427–436.
41. Wittenburg H, Carey MC. Biliary cholesterol secretion by the twinned sterol half-transporters ABCG5 and ABCG8. J Clin Invest 2002;110:605–609.

Received July 20, 2010. Accepted January 18, 2011.

Reprint requests

Address requests for reprints to: Tappei Takada, PhD, Department of Pharmacy, The University of Tokyo Hospital, Faculty of Medicine, The University of Tokyo, 7-3-1 Hongo, Bunkyo-ku, Tokyo 113-8655, Japan. e-mail: tappei-tky@umin.ac.jp; fax: (81) 3-3816-6159.

Acknowledgments

Yoshihide Yamanashi and Tappei Takada contributed equally to this study.

Conflicts of interest

The authors disclose no conflicts.

Funding

Supported by grants from the Ministry of Education, Culture, Sports, Science and Technology of Japan and Grant-in-Aid for Scientific Research on Innovative Areas HD-physiology (22136015).

J Gastroenterol (2011) 46:779–789
DOI 10.1007/s00535-011-0380-3

ORIGINAL ARTICLE—LIVER, PANCREAS, AND BILIARY TRACT

Potent in vitro and in vivo antitumor activity of sorafenib against human intrahepatic cholangiocarcinoma cells

Hiroaki Sugiyama · Kenichiro Onuki · Kazunori Ishige · Nobue Baba · Tetsuya Ueda · Sachiko Matsuda · Kaoru Takeuchi · Masafumi Onodera · Yasuni Nakanuma · Masayuki Yamato · Masakazu Yamamoto · Ichinosuke Hyodo · Junichi Shoda

Received: 2 November 2010 / Accepted: 20 January 2011 / Published online: 18 February 2011
© Springer 2011

Abstract
Background Intrahepatic cholangiocarcinoma (ICC) is rising in clinical importance due to the increasing incidence worldwide, poor prognosis, and suboptimal response to therapies. New effective therapeutic approaches are needed for improvement of treatment outcome. A recent study showed that sorafenib, a multikinase inhibitor that acts predominantly through inhibition of Raf kinase and vascular endothelial growth factor (VEGF) and platelet-derived growth factor (PDGF) receptors, exhibited potent antitumor activity in a preclinical model of cholangiocarcinoma cells.
Method We tested the in vitro and in vivo antitumor activity of sorafenib against human ICC cell lines.
Results Treatment of ICC cells with sorafenib resulted in inhibition of proliferation and induction of apoptosis in the cell lines. In the cells treated with sorafenib, phosphorylation of mitogen-activated protein kinase kinase (MEK) and mitogen-activated protein kinase (MAPK) and also interleukin-6-induced phosphorylation of signal transducer and activator of transcription 3 (STAT3) were inhibited in a dose-dependent manner. Down-regulation of the anti-apoptotic protein myeloid cell leukemia-1 (Mcl-1) paralleled the reduced phosphorylation of STAT3. However, sorafenib induced no significant change in the cell cycle distribution and the expression levels of cyclin D1 and $p27^{Kip1}$ in the cells. For the in vivo antitumor activity, oral administration of sorafenib significantly inhibited the growth of subcutaneous tumors established in immunodeficient mice at doses of 10, 30, and 100 mg/kg. Moreover, administration of sorafenib (30 mg/kg) to animals with peritoneally disseminated ICC resulted in significantly

H. Sugiyama · K. Ishige · I. Hyodo · J. Shoda
Department of Gastroenterology, Institute of Clinical Medicine, University of Tsukuba Graduate School of Comprehensive Human Sciences, Tsukuba, Ibaraki, Japan

K. Onuki · M. Yamamoto
Department of Surgery, Institute of Gastroenterology, Tokyo Women's Medical University, Shinjuku-ku, Tokyo, Japan

N. Baba · T. Ueda
Pharmacodynamics Group, Drug Development Service Division, Medi-Chem Business Segment, Itabashi-ku, Tokyo, Japan

S. Matsuda
Department of Surgery, School of Medicine, Keio University, Shinjuku-ku, Tokyo, Japan

K. Takeuchi
Department of Infection Biology, Institute of Basic Medical Science, University of Tsukuba Graduate School of Comprehensive Human Sciences, Tsukuba, Ibaraki, Japan

M. Onodera
Department of Genetics, National Research Institute for Child Health and Development, Setagaya-ku, Tokyo, Japan

Y. Nakanuma
Department of Human Pathology, Graduate School of Medical Science, Kanazawa University, Kanazawa, Japan

M. Yamato
Institute of Advanced Biomedical Engineering and Science, Tokyo Women's Medical University, Shinjuku-ku, Tokyo, Japan

J. Shoda (✉)
Field of Basic Sports Medicine, Sports Medicine, University of Tsukuba Graduate School of Comprehensive Human Sciences, Tsukuba, Ibaraki, Japan
e-mail: shodaj@md.tsukuba.ac.jp

prolonged survival compared with that of untreated animals (76 vs. 43 days in treated and vehicle-treated mice, respectively).
Conclusion These results indicate that sorafenib is a potent agent that may provide a new therapeutic option for human ICC.

Keywords Cholangiocarcinoma · Molecular targeting therapy · Multi-tyrosine kinase inhibitor · Antitumor activity · Preclinical study

Abbreviations

Ab	Antibody
AKT/PKB	Protein kinase B
CC	Cholangiocarcinoma
IH	Intrahepatic
IL-6	Interleukin-6
JAK	Janus kinase
MAPK	Mitogen-activated protein kinase
Mcl-1	Myeloid cell leukemia-1
MEK	Mitogen-activated protein kinase kinase
STAT	Signal transducer and activator of transcription

Introduction

The incidence and mortality rates for intrahepatic cholangiocarcinoma (ICC) have been steadily increasing worldwide, with notable increases being reported in the USA, the UK, and Asia including Japan [1, 2]. Known risk factors are primary sclerosing cholangitis, liver fluke infestations, and hepatolithiasis [2]. Recent studies suggested that chronic hepatitis C infection and non-alcoholic steatohepatitis, especially when combined with cirrhosis, also contribute to cholangiocarcinogenesis in the intrahepatic bile ducts [3]. However, the reason for the increasing incidence of ICC remains unclear.

Despite advances in tumor biology, diagnostic imaging, adjuvant therapies, and surgical techniques, the survival of ICC patients remains dismal [4, 5]. Without early resection, these tumors invade adjacent vascular structures and liver parenchyma, extend along the bile duct epithelia, metastasize to the lymph nodes, and disseminate into the peritoneal space. The mainstay of treatment for ICC is complete resection with negative surgical margins. Under these circumstances, however, the role of adjuvant therapy is not well defined, and the benefits of palliative chemotherapy or chemoradiation for patients with unresectable disease have not been established. An effective new approach against this aggressive disease is urgently needed.

Recently, a number of multi-targeted tyrosine kinase inhibitors have been developed and used in clinical trials for cancer therapy [6]. Sorafenib (BAY43-9006, Nexavar) is an oral multikinase inhibitor that was developed as a c-Raf kinase inhibitor. It also targets several other Raf kinases as well as receptor tyrosine kinases such as vascular endothelial growth factor receptor (VEGFR) and platelet-derived growth factor receptor (PDGFR) [7]. Sorafenib has shown potent antitumor activity in vitro and in vivo in a broad range of malignancies including renal cell, hepatocellular, breast, colon, pancreas, and ovarian carcinomas [8, 9]. On the basis of the results of the SHARP study [10], sorafenib was approved for treatment of unresectable hepatocellular carcinoma (HCC) cases. A phase II trial of single-agent sorafenib in patients with advanced biliary tract carcinoma has been conducted [11]. In addition, sorafenib was recently reported to exert in vitro antitumor activity against human cholangiocarcinoma through blockage of growth factor-induced activation of the mitogen-activated protein kinase (MAPK) pathway and cell cycle arrest [12]. Sorafenib therefore merits further in vitro and in vivo evaluations to explore the mechanisms and molecular pathways involved in the observed antitumor activity in a panel of human ICC cell lines.

In this study, the in vitro and in vivo tumor activity of sorafenib was assessed in preclinical models using human ICC cell lines with focus on (1) the molecular mechanisms responsible for the observed tumor growth inhibition and apoptosis induction and (2) whether ICC is targeted in vivo in animals bearing subcutaneously (s.c.) growing xenografted tumors or peritoneally disseminated ICC tumors. Treatment with sorafenib resulted in inhibition of MEK and MAPK phosphorylation as well as interleukin-6-induced phosphorylation of signal transducer and activator of transcription 3 (STAT3) in ICC cells. Down-regulation of the anti-apoptotic protein myeloid cell leukemia-1 (Mcl-1) paralleled the reduced phosphorylation of STAT3. Administration of a tolerable dose of sorafenib induced significant regression of established ICC tumors and significantly improved the survival of animals with disseminated tumors.

Materials and methods

Cell line and animals

The experiments were performed on 8 human ICC cell lines: YSCCC and HuH-28 from RIKEN Cell Bank (Ibaraki, Japan), HuCCT-1 from the Health Science Research Resources Bank (Osaka, Japan), KMC-1 and KMCH-1 [13, 14] from Dr. M. Kojiro (Kurume University School of Medicine, Kurume, Japan), CCKS-1 [15] from

Dr. Y. Nakanuma (Kanazawa University Graduate School, Kanazawa, Japan), and KKU-100 and KKU-M214 [16, 17] from Dr. B. Sripa (Khon Kaen University, Thailand). In addition, PLC/PRF/5, a human hepatocellular carcinoma cell line, was obtained from the American Type Culture Collection (Rockville, MD). CCKS-1 cells were cultured in RPMI 1640 medium and other cell lines were cultured in Dulbecco's modified Eagle's medium (DMEM) containing 10% heat-inactivated fetal calf serum (Invitrogen, Carlsbad, CA, USA) in a humidified atmosphere with 5% CO_2 at 37°C. To establish KKU-100 cells expressing luciferase (KKU-100-luc), an *Xho*I–*Bam*HI fragment containing a full-length luciferase cDNA was inserted into the corresponding site of GCDNsamIRES/EGFP [18], which was referred to as pGCDNsamLucI/E. The vector was converted to the corresponding retrovirus by transduction into 293gpg as described elsewhere [19]. KKU-100 cells were infected with retrovirus GCDNsamLucI/E. The expression level of luciferase was confirmed by using a luciferase assay reagent (Promega, Madison, WI, USA). Four-week-old female BALB/c nu/nu athymic mice were purchased from Sankyo Labo Service (Tokyo, Japan). All animal experiments were approved by the Institutional Animal Care and Use Committee of Tokyo Women's Medical University.

Sorafenib (Nexavar™)

Sorafenib tosylate was provided by Bayer Schering Pharma (Leverkusen, Germany). For in vitro administration, sorafenib was dissolved in dimethyl sulfoxide (DMSO) to a concentration of 10 mmol/L and further diluted to an appropriate final concentration in fresh media. In all experiments, the final DMSO concentration did not exceed 0.1%, thus not affecting cell growth. For in vivo administration, sorafenib was dissolved in Cremophor EL/ethanol (50:50; Sigma Cremophor EL, 95% ethanol) and handled as described previously [7].

Cell viability assay

The in vitro effect of sorafenib on growth inhibition of ICC cell lines was determined by a cell viability assay using a WST-8 reduction assay kit (Dojin Laboratories, Tokyo, Japan) according to the manufacturer's instructions. Cells were plated at 5,000 per well in 96-well microtiter plates and incubated overnight. On the following day, various concentrations of sorafenib were added to the wells and the cells were incubated for an additional 72 h. WST-8 was added and cell viability was determined by reading optical density values from a microplate reader at an absorption wavelength of 450 nm. All assays were performed twice. The IC_{50} value, at which 50% cell growth inhibition compared with that of the DMSO control was obtained, was calculated.

Annexin V apoptosis assay

Cells were cultured in 6-well plates at 3×10^5 cells per well. On the following day, the cells were treated with sorafenib at concentrations of 0, 5, 10, and 15 μmol/L for 24 or 48 h. After the treatment, both detached and attached cells were collected and apoptotic cells were detected by using an Annexin V-FITC Apoptosis Detection Kit (Beckman Coulter). The cells were stained with Annexin V-FITC and propidium iodide (PI) according to the manufacturer's instructions. The apoptotic fraction was identified as Annexin V-positive and PI-negative cells using a FACS Calibur (Becton–Dickinson, San Jose, CA, USA). All assays were performed in quadruplicate.

Terminal dUTP nick-end labeling (TUNEL) assay

Cells were cultured on chamber slides and allowed to adhere overnight, and they were then treated with sorafenib at concentrations of 0, 5, 10, and 15 μmol/L for 24 h. Apoptosis of the cells was evaluated on the basis of the TUNEL assay using the Dead End Fluorometric TUNEL System (Promega, Madison, WI, USA) according to the manufacturer's instructions. All assays were performed in quadruplicate.

Cell cycle analysis

Cells were cultured in 6-well plates at 3×10^5 cells per well. On the following day, the cells were treated with sorafenib at concentrations of 0, 3, 10, and 15 μmol/L for 24 h. After the treatment, the cell nuclei were isolated using CycleTest PLUS DNA Reagent Kit (Becton–Dickinson). The DNA was stained with PI according to the manufacturer's instructions. The stained DNA was analyzed by a FACS Calibur and the DNA content was quantified using ModFit software (Verity Software House, Topsham, ME, USA). All assays were performed in quadruplicate.

Immunoblot analysis

After treatment, whole-cell lysates were prepared as previously described [20]. Aliquots of cell lysate were loaded on 4–12% gradient sodium dodecyl sulfate polyacrylamide gel electrophoresis (SDS-PAGE) gel, electrophoresed under reducing conditions, and transferred onto a poly(vinylidene difluoride) (PVDF) membrane. Blots were probed with an antibody raised against MAPK, phospho-MAPK (Erk1/2) (Thr^{202}/Tyr^{204}), MEK, phospho-MEK

(Ser^{221}), STAT3, phospho-STAT3 (Tyr^{705}), AKT, phospho-AKT (Ser^{473}), Mcl-1, Bcl-xl, caspase-3, cyclin-dependent kinase inhibitor p27^{kip1} (Cell Signaling Technology Inc, Beverly, MA, USA), cyclin-dependent kinase cyclin D1 (Abcam, Cambridge, MA, USA), or β-actin (Sigma-Aldrich, St. Louis, MO, USA). Proteins were visualized on Hyperfilm^{TM} using an ECL/western blotting system (GE Healthcare, Piscataway, NJ, USA) according to the manufacturer's instructions. β-Actin was used as the internal control. In some experiments, KKU-100 and KMCH-1 cells were treated with 5 or 10 μmol/L sorafenib for 24 h. In the last 10 min of the incubation period with the drug, cells were stimulated with IL-6 (10 ng/ml). The cell lysates were prepared in the same way as described above and subjected to immunoblotting for STAT3, pSTAT3, and Mcl-1.

Subcutaneous xenografted ICC tumor model

An s.c. xenografted model injected with KKU-100 cells was prepared as previously described [20]. Sorafenib was administered orally once daily for 21 days at doses of 10, 30, and 100 mg/kg body weight. Treatment was initiated when tumor volumes reached median sizes of 140–180 mm^3 with 8 mice per group. Body weights and tumor volume were measured twice weekly starting on the first day of treatment. Tumor size was measured using Vernier calipers and tumor volume was calculated as 0.5 × longest diameter × width^2. The percentage of tumor inhibition was calculated according to the formula $[1 - (T/C)] \times 100$, where T and C represent the mean tumor volumes of the treatment group and the control group, respectively. In some experiments, animals with tumors measuring 150–300 mm^3 in size were administered sorafenib orally once daily for 5 days at doses of 30 and 100 mg/kg. Tumors were harvested 3 h after the last treatment and either homogenized in lysis buffer for immunoblot analysis or fixed in paraformaldehyde and paraffin-embedded. Immunohistochemical staining of tumors was done with a monoclonal Ab raised against CD31 (Abcam). TUNEL staining for tumor tissue was based on the protocol of the Dead End Colorimetric TUNEL System (Promega). The tissue sections were viewed at ×100 magnification and images were captured with a digital camera. Four fields per section were analyzed, excluding peripheral connective tissue and necrotic regions. Microvessel density (MVD) in each field was defined as the mean number of microvessels containing high levels of CD31-stained microvessels. Percentage of apoptotic cells was defined as TUNEL-positive cells among 1000 tumor cells. Mean values of MVD and percentage of TUNEL-positive cells in each group were calculated from three tumor specimens.

Intraperitoneally disseminated ICC tumor model

An intraperitoneal (i.p.) dissemination model injected with KKU-100-luc cells was prepared as previously described [20]. Five days after tumor cell injection, establishment of intraperitoneally disseminated ICC was confirmed by injection of luciferin and imaging of photon emission. The mice were randomized into 3 groups: vehicle control or daily administration of sorafenib at 10 or 30 mg/kg with 8 mice per group. Mice were weighed twice weekly and killed if they had lost more than 20% of body weight or seemed moribund. The mice were treated for 46 days, and photon counting was conducted one or two times a week. Bioluminescence images were used to monitor the dynamics of peritoneal tumor growth. Immediately before imaging, 150 mg/kg of D-luciferin (Alameda, CA, USA) was administered to mice by i.p. injection. After 15 min, photons from whole bodies were counted using the IVIS imaging system (Xenogen) in accordance with the manufacturer's instructions. Total flux (photons/s) of emitted light was used as a measure of the relative number of viable tumor cells in the peritoneal tumor. Data were analyzed using Living Image 3.0 software (Xenogen).

Statistical analysis

Values are given as mean ± SD (standard deviation). Statistical evaluations of data were analyzed using one-way analysis of variance (ANOVA) followed by the Tukey–Kramer test. The survival of animals in the peritoneal dissemination model was analyzed using the Kaplan–Meier method. Differences in the survival of animals in subgroups were analyzed by the log-rank test. A P value of less than 0.05 was defined as statistically significant.

Results

Sorafenib inhibits proliferation of ICC cells

Treatment of ICC cells with sorafenib for 72 h resulted in potent growth inhibition in a dose-dependent manner for all of the 8 cell lines studied (Fig. 1). The IC_{50} of sorafenib ranged from 3.8 to 10.3 μmol/L. KKU-100 was found to be most sensitive and HuH-28 least sensitive to the drug. In terms of the IC_{50} value, five of the 8 ICC cell lines studied were comparable to PLC/PRF/5, a human HCC cell line (IC_{50} 7.0 ± 0.3 μmol/L).

Sorafenib induces apoptosis in ICC cells

Four ICC cell lines, KKU-100, KMCH-1, HuCCT-1, and CCKS-1, were treated with sorafenib at concentrations of

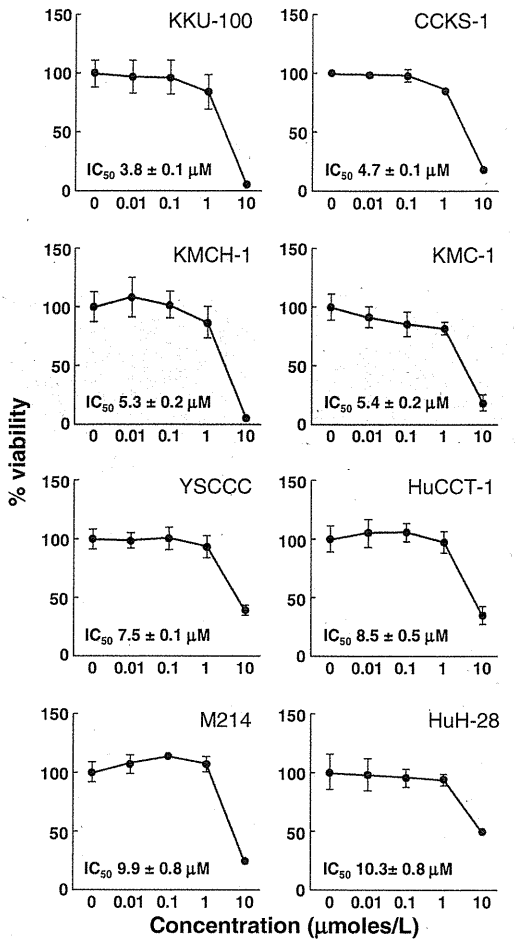

Fig. 1 In vitro growth inhibition of ICC cells cultured with sorafenib. Eight ICC cell lines (5×10^3 cells) were cultured in DMEM or RPMI 1640 medium with various concentrations of sorafenib (0–10 μmol/L) for 72 h at 37°C. Growth inhibition data are given as percentages of the viability of cells cultured without the drug. The results are presented as mean ± SD of sextuplicate determinations. The assay was repeated twice

5, 10, and 15 μmol/L for 24 and 48 h. In flow cytometry analysis, the proportion of annexin V-positive and PI-negative cells was increased in a dose-dependent and time-dependent manner for all of the 4 ICC cell lines studied (Fig. 2a). Similar to the results of flow cytometry analysis, in the TUNEL assay (Figs. 2b, c), the percentages of TUNEL-positive cells in the 4 ICC cell lines were 1.9–3.8% without treatment and 4–8% with 5 μmol/L, 8–12% with 10 μmol/L, and 10–17% with 15 μmol/L sorafenib treatment for 24 h.

Sorafenib induces no cell cycle arrest

Three ICC cell lines, KKU-100, KMCH-1, and HuCCT-1, were treated with sorafenib at concentrations of 3, 10, and 15 μmol/L for 24 h. The cell cycle analysis by flow cytometry showed that the sorafenib treatment for 24 h did not cause any significant changes in the cell cycle distribution in these cells (Fig. 3). The cell cycle arrest, that is, the increase in the G_1 phase and the decrease in the S phase, was not observed in these cells (Fig. 3a). Supporting this observation, the immunoblot analysis revealed that the treatment did not induce any changes in the expression levels of the cell cycle promoter cyclin D1 and the cell cycle inhibitor $p27^{Kip1}$ (Fig. 3b), both of which are important for cell cycle regulation [21, 22].

Sorafenib inhibits the RAF/MEK/MAPK signaling pathway in ICC cells

Following the observation that sorafenib inhibits the RAF/MEK/MAPK signaling pathway in a number of tumors, this inhibitory effect of the drug was investigated for 2 ICC cell lines, KKU-100 and KMCH-1. By treatment at concentrations of 2.5–10 μmol/L, hyperphosphorylation of MEK and MAPK was inhibited in these cells (Fig. 4a). However, hyperphosphorylation of AKT, a signaling molecule on the PI3 kinase pathway, was not inhibited (Fig. 4a).

Sorafenib reduces STAT3 and Mcl-1 expression levels

In human cholangiocarcinoma cells, sorafenib was recently shown to inhibit the JAK/STAT3 signaling axis at the level of STAT3 phosphorylation, leading to down-regulation of Mcl-1, an anti-apoptotic protein [23]. Therefore, this inhibitory effect of the drug was investigated for KKU-100 and KMCH-1 cells. By treatment at concentrations of 2.5–10 μmol/L, hyperphosphorylation of STAT3 was inhibited in these cells (Fig. 4b). Expression of the anti-apoptotic protein Mcl-1, but not that of Bcl-xL, was potently down-regulated in the cells (Fig. 4b). Moreover, cleavage of caspase-3, which is reportedly found in apoptotic cells, was detected in cells treated at a concentration of 10 μmol/L. These results are consistent with the induction of apoptosis by sorafenib through a down-regulation of Mcl-1, which may be independent of the inhibitory effects on MEK/MAPK signaling. As shown in Fig. 4c, in KKU-100 and KMCH-1 cells, interleukin-6 (IL-6)-stimulated phosphorylation of STAT3 was inhibited by sorafenib at a concentration of 10 μmol/L. Sorafenib also decreased Mcl-1 levels in the presence of IL-6 (Fig. 4c). Because the IL-6/STAT3 pathway is known to control Mcl-1 transcription in human ICC [24], the inhibition of IL-6-induced STAT3 activation by sorafenib may be one mechanism by which sorafenib exerts potent antitumor activity against human ICC cells.

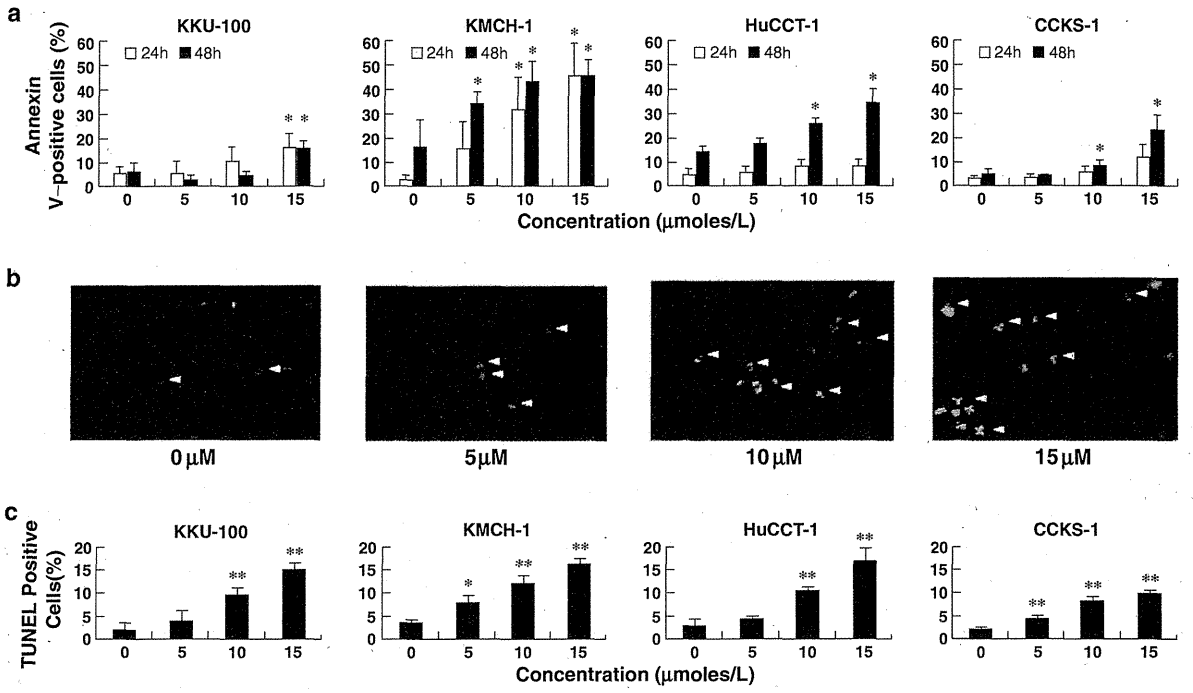

Fig. 2 Induction of apoptosis in ICC cells by sorafenib. **a** ICC cells were treated with various concentrations of sorafenib (0–15 μmol/L) for 24 and 48 h at 37°C. The apoptotic fraction identified as Annexin V-positive and PI-negative cells was determined by flow cytometric analysis. **b** TUNEL staining was done for ICC cells (KKU-100, KMCH-1, HuCCT-1, and CCKS-1 cells) treated with sorafenib for 24 h. *Green* nuclear staining indicates apoptotic cells. **c** The percentage of TUNEL-positive cells was quantified for each cell line. *Columns* and *error bars* represent means of three independent determinations and SD, respectively. Significant differences between the DMSO controls and the treatment groups are indicated by $*P < 0.05$ or $**P < 0.01$. All assays were performed in quadruplicate

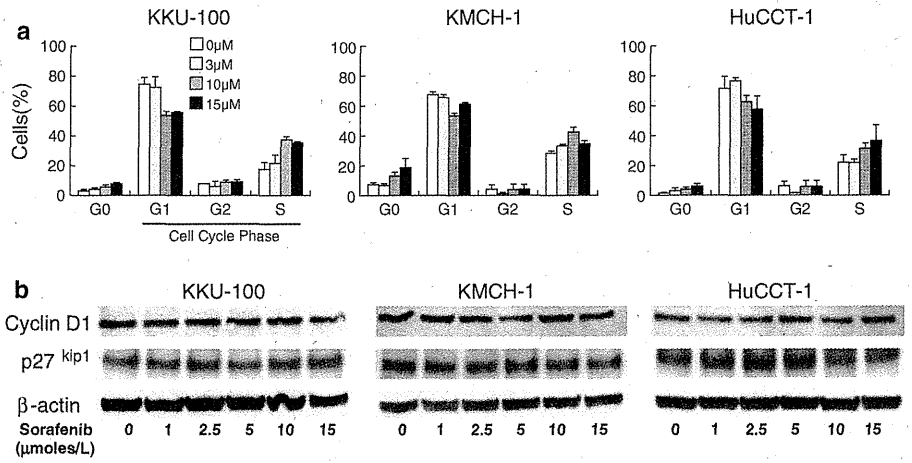

Fig. 3 Effects of sorafenib on cell cycle distribution in ICC cells (KKU-100, KMCH-1, and HuCCT-1). **a** ICC cells were treated with various concentrations of sorafenib (0–15 μmol/L) for 24 h at 37°C. After the treatment, the cell nuclei were isolated and stained with PI. The stained DNA was analyzed by flow cytometry, and then the DNA content was quantified. **b** Immunoblot analysis of cell cycle promoter cyclin D1 and the cell cycle inhibitor $p27^{Kip1}$ in the cells. The cells were treated with various concentrations of sorafenib (0–15 μmol/L) for 24 h

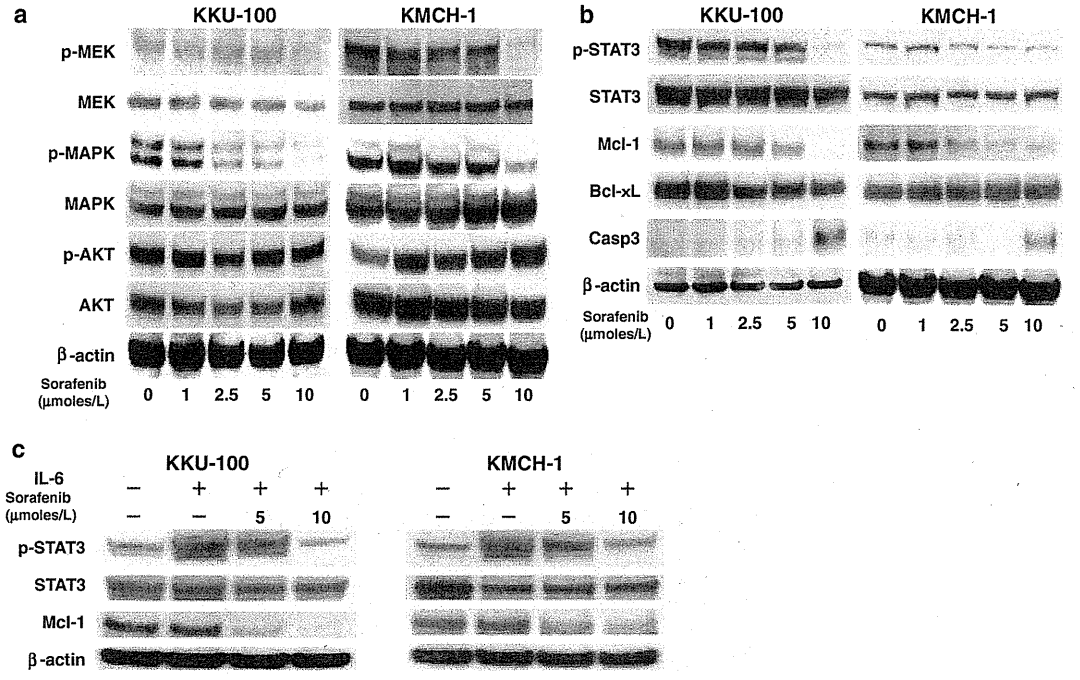

Fig. 4 Effects of sorafenib on expression of cell signaling molecules and apoptosis-related molecules in ICC cells (KKU-100 and KMCH-1 cells). **a** Immunoblot analysis of cell signaling molecules, MEK, MAPK, and Akt. The cells were treated with various concentrations of sorafenib (0–10 μmol/L) for 4 h. **b** Immunoblot analysis of cell signaling molecule STAT3 and apoptosis-related molecules, Mcl-1, Bcl-xL, and cleaved caspase-3, in the cells. The cells were treated with various concentrations of sorafenib (0–10 μmol/L) for 24 h. **c** Immunoblot analysis of STAT3 and Mcl-1 in the cells with and without IL-6 stimulation in the sorafenib treatment. The cells were treated with various concentrations of sorafenib (0–10 μmol/L) for 24 h and then stimulated with IL-6 for 10 min. Each protein was normalized to β-actin

In vivo antitumor activity of sorafenib against s.c. xenografted ICC tumors

Following the observation of potent antitumor activity in vitro, the in vivo antitumor activity of sorafenib was studied using s.c. tumor-bearing mice. As shown in Fig. 5a, sorafenib inhibited growth of s.c. xenografted tumors at all doses tested. Compared with the vehicle-treated group, mice treated with 10, 30, and 100 mg/kg sorafenib showed 44, 75, and 84% inhibition of tumor growth on day 16 after the start of treatment, respectively ($P < 0.001$). No evidence of toxicity, as determined by increased weight loss relative to control animals or drug-related lethality, was observed in any of the groups. As shown in Fig. 5b, in the s.c. xenografted tumors of mice treated with sorafenib, the expression levels of pMAPK and pSTAT3 and that of Mcl-1 were decreased, whereas the level of cleaved caspase-3 was increased. Moreover, MVD was significantly decreased in tumor specimens from sorafenib-treated groups compared with that in specimens from the vehicle-treated group, as assessed by CD31 staining (Fig. 5c). Figure 5c also shows that sorafenib induced tumor cell apoptosis as measured by TUNEL staining at both doses evaluated. The reduction in MVD and increase in TUNEL-positive staining are quantified in graphs shown in Fig. 5d. MVD was reduced from 28.8 counts/field in the vehicle-treated group to 11.3 and 5 counts/field in the groups treated with 30 and 100 mg/kg sorafenib, respectively. TUNEL staining in the same samples was increased from 1.7% positive area in the vehicle-treated group to 8.7 and 11.6% positive areas in the groups treated with 30 and 100 mg/kg sorafenib, respectively.

In vivo antitumor activity of sorafenib against peritoneally disseminated ICC tumors

To mimic the clinical aggressiveness of ICC, a peritoneally disseminated tumor model was developed using immunodeficient mice that were inoculated with KKU-100-luc cells into the peritoneal cavity. Five days after cell implantation, establishment of peritoneally disseminated ICC was confirmed using IVIS (Fig. 6a). After administration of sorafenib, tumor volume in the intraperitoneal cavity was assessed using the IVIS imaging system that visualizes viable tumor cells as photon intensity (Fig. 6b). The intensity of light-emitting signals is depicted according

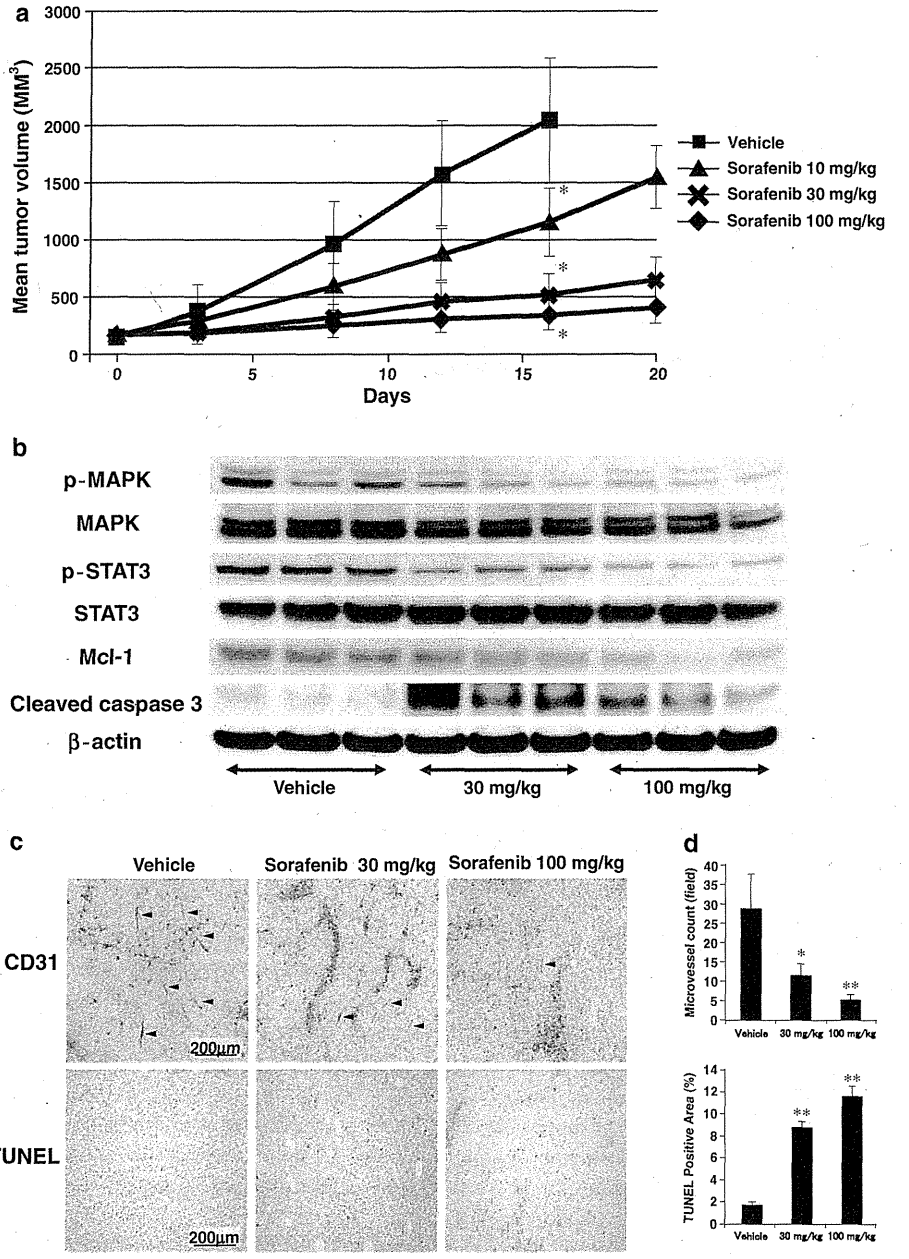

Fig. 5 In vivo antitumor activity of sorafenib against s.c. xenografted tumors of ICC cells in mice. **a** Subcutaneous tumors were seeded in immunodeficient mice using KKU-100 cells, as described in the "Materials and methods". Each group consisted of 8 animals. Tumor volumes were measured two or three times a week, and tumor volume (mm^3) was calculated as 0.5 × longest diameter × width^2. Tumor volumes are presented as mean ± SD of 8 mice for each group. The mice in vehicle-treated group had to be euthanized on day 16 due to tumor burden. Significant differences between the treatment groups and vehicle-treated group are indicated by $^*P < 0.01$. A significant reduction in tumor volume was observed in a dose-dependent manner in mice in the sorafenib groups 16 days after the start of treatment. **b** Immunoblot analysis of MAPK, STAT3, Mcl-1, and cleaved caspase-3 in the tumors. Each protein was normalized to β-actin. Tumor samples from 3 representative animals from each group are shown. **c** CD31 staining and TUNEL staining in the tumors. **d** Quantification of microvessel (assessed by CD31 staining) and TUNEL-positive cells from immunohistochemical analysis of the tumors. *Columns* and *error bars* represent means and SD of the values of MVD and those of TUNEL-positive cells in each group, respectively. Significant differences between the treatment groups and vehicle-treated group are indicated by $^*P < 0.05$ or $^{**}P < 0.01$

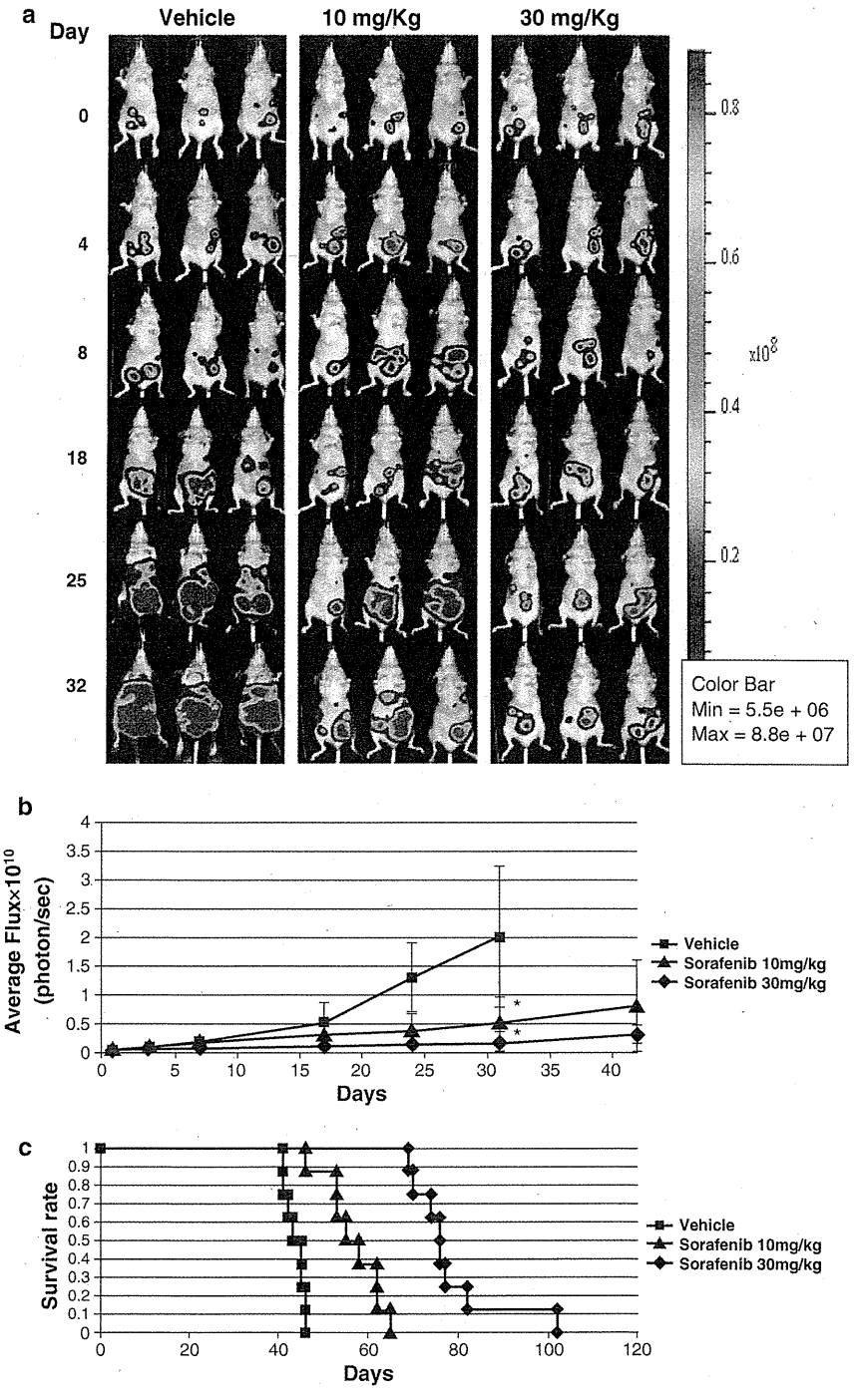

Fig. 6 In vivo antitumor activity of sorafenib against peritoneally disseminated tumors of ICC cells in mice. Peritoneally disseminated tumors were seeded in immunodeficient mice using KKU-100-luc cells (5×10^6 cells/mouse), as described in the "Materials and methods". Each group consisted of 8 animals. **a** Sequential in vivo whole-body imaging of tumor progression over time. Bioluminescence images facilitated real-time visualization of tumor burden in live animals. *Panels* depict three representative mice from each of the vehicle- and sorafenib-treated (10 and 30 mg/kg body weight) groups. Images were captured every other day after the treatment started. **b** Time course of changes in quantification of tumor bioluminescence. *Points* represent the mean area of bioluminescence for live intact animals in each treatment group ($n = 8$ mice); *error bars*, SD. Significant differences between the treatment groups and vehicle-treated group are indicated by $^*P < 0.01$. **c** Relationship between survival outcome and sorafenib treatment in mice with peritoneally disseminated tumors of ICC cells as assessed using Kaplan–Meier survival curves. The median survival period in the vehicle group was 43 days, and the mean survival periods in the groups treated with sorafenib at doses of 10 and 30 mg/kg body weight were 55 and 76 days, respectively. The difference was statistically significant ($P < 0.005$)

to the color bar in Fig. 6a. The blue area indicates small amounts of tumor, whereas the red area indicates large amounts of tumor. In stark contrast to the vehicle group where the intensity and area of light emission increased over time, those of the 10 and 30 mg/kg sorafenib-treated groups decreased over time. On day 31 after the start of treatment, the average photon intensity (total flux) was significantly decreased in the treated groups compared with that in the vehicle-treated group ($P < 0.001$). In addition, as shown in Fig. 6c, the median survival periods in the treated groups at doses of 10 and 30 mg/kg were 55 and 76 days, respectively, which were significantly longer than the survival period of 43 days in the vehicle-treated group ($P < 0.005$).

Discussion

Therapeutic options for ICC are unsatisfactory, and the survival outcome is therefore poor. Effective therapeutic approaches against this aggressive disease are urgently needed. Sorafenib was recently approved for treatment of advanced HCC on the basis of positive results of a large phase III randomized clinical trial [10]. Following the positive results for treatment of HCC, the efficacy of this drug against human ICC, a more aggressive disease, was evaluated in preclinical models in this study.

We demonstrated in the human ICC cell lines that sorafenib blocks phosphorylation of MEK/MAPK, and IL-6-stimulated phosphorylation of STAT3, causes down-regulation of Mcl-1, inhibits tumor cell proliferation, and induces apoptosis in vitro. However, in stark contrast to the result of a recent study [12], sorafenib-induced cell cycle arrest (i.e., arrest in the G_1 phase) was not seen in any of the human ICC cell lines that we utilized in this study, in which induction of expression of the cell cycle inhibitor $p27^{Kip1}$ and suppression of the cell cycle promoter cyclin D1 were not observed. Consistent with the observation in this study, a previous study [12, 25] reported that sorafenib-induced cell cycle arrest was not seen in PLC/PRF/5, a human HCC cell line, and EGI-1, a human ICC cell line. Nevertheless, sorafenib exhibited robust in vivo antitumor efficacy, including partial tumor regressions in both an s.c. xenografted tumor model and a peritoneally disseminated tumor model. Moreover, in animals treated with sorafenib, a significant reduction in MVD (tumor angiogenesis) measured by CD31 staining was observed in s.c. xenografted tumors. Collectively, these results provide evidence that sorafenib may be an attractive agent for treatment of ICC by simultaneously inhibiting both tumor angiogenesis (VEGF and PDGF signaling) and tumor cell survival (RAF kinase signaling-dependent and STAT3 signaling-dependent mechanisms) rather than by inducing tumor cell cycle arrest.

In ICC, inflammation-associated carcinogenesis is, in part, mediated by dysregulated cytokine signaling pathways [26], which potentially can be therapeutically targeted for treatment of this cancer. Members of the STAT family are key signal transducers in cytokine and growth factor signaling. STAT3 has been shown to be an essential signaling molecule in cholangiocarcinogenesis through its transcriptional activity on genes regulating apoptosis, proliferation, differentiation, and angiogenesis [27, 28]. One of the main activators of STAT3 in ICC cells is IL-6 via JAK [29]. IL-6 is a cytokine secreted by inflammatory cells (i.e., macrophages) but also by ICC cells, where it activates STAT3 by autocrine and paracrine mechanisms [24, 30–32]. Activation of STAT3 transcriptionally targets Mcl-1, an anti-apoptotic Bcl-2 family protein [24]. The results of this study support results recently reported by Blechacz et al. [23] showing that sorafenib inhibits the JAK/STAT3 signaling axis at the level of STAT3 phosphorylation, resulting in down-regulation of Mcl-1, thereby sensitizing human ICC cells to apoptosis.

Sorafenib exhibited significant antitumor activity against ICC tumors in the peritoneal metastasis model. In the clinical course of ICC, peritoneal dissemination is a very unfavorable development that frequently occurs in patients with advanced ICC. Since systemic chemotherapy using anticancer drugs has shown few significant benefits for patients with advanced ICC (e.g., peritoneally disseminated ICC) [33, 34], administration of sorafenib may be a useful option.

In summary, this study showed that sorafenib induces inhibition of the RAF/MEK/MAPK signaling pathway, reduction of STAT3 phosphorylation, and down-regulation of Mcl-1 protein level, all of which may contribute to the pro-apoptotic effects of the drug and also to the pronounced antivascular effects in in vitro and in vivo models using human ICC cells. A recent preclinical study provided a rationale for sorafenib's suitability for combination therapy with chemotherapeutic agents [12]. The results of this study may provide a rationale for a monotherapeutic approach against ICC by sorafenib or for the use of sorafenib in combination with other chemotherapeutic agents, and the results indicate the need for a phase II or III clinical trial.

Acknowledgments This work was supported in part by Grants-in-Aid for Scientific Research from the Ministry of Education, Culture, Sports, Science and Technology, Japan (20390339, 22390379, 22591530).

Conflict of interest All authors declare that they have no conflict of interests or financial interests.

References

1. Blechacz B, Gores GJ. Cholangiocarcinoma: advances in pathogenesis, diagnosis, and treatment. Hepatology. 2008;48:308–21.
2. Khan SA, Thomas HC, Davidson BR, Taylor-Robinson SD. Cholangiocarcinoma. Lancet. 2005;366:1303–14.
3. Lazaridis KN, Gores GJ. Cholangiocarcinoma. Gastroenterology. 2005;128:1655–67.
4. Jarnagin WR, Fong Y, DeMatteo RP, Gonen M, Burke EC, Bodniewicz BJ, et al. Staging, resectability, and outcome in 225 patients with hilar cholangiocarcinoma. Ann Surg. 2001;234:507–17 (discussion 517–9).
5. Huang JL, Biehl TR, Lee FT, Zimmer PW, Ryan JA Jr. Outcomes after resection of cholangiocellular carcinoma. Am J Surg. 2004;187:612–7.
6. Tabernero J. The role of VEGF and EGFR inhibition: implications for combining anti-VEGF and anti-EGFR agents. Mol Cancer Res. 2007;5:203–20.
7. Wilhelm SM, Carter C, Tang L, Wilkie D, McNabola A, Rong H, et al. BAY 43–9006 exhibits broad spectrum oral antitumor

activity and targets the RAF/MEK/ERK pathway and receptor tyrosine kinases involved in tumor progression and angiogenesis. Cancer Res. 2004;64:7099–109.
8. Wilhelm SM, Adnane L, Newell P, Villanueva A, Llovet JM, Lynch M. Preclinical overview of sorafenib, a multikinase inhibitor that targets both Raf and VEGF and PDGF receptor tyrosine kinase signaling. Mol Cancer Ther. 2008;7:3129–40.
9. Strumberg D, Richly H, Hilger RA, Schleucher N, Korfee S, Tewes M, et al. Phase I clinical and pharmacokinetic study of the Novel Raf kinase and vascular endothelial growth factor receptor inhibitor BAY 43-9006 in patients with advanced refractory solid tumors. J Clin Oncol. 2005;23:965–72.
10. Llovet JM, Ricci S, Mazzaferro V, Hilgard P, Gane E, Blanc JF, et al. Sorafenib in advanced hepatocellular carcinoma. N Engl J Med. 2008;359:378–90.
11. Bengala C, Bertolini F, Malavasi N, Boni C, Aitini E, Dealis C, et al. Sorafenib in patients with advanced biliary tract carcinoma: a phase II trial. Br J Cancer. 2010;102:68–72.
12. Huether A, Hopfner M, Baradari V, Schuppan D, Scherubl H. Sorafenib alone or as combination therapy for growth control of cholangiocarcinoma. Biochem Pharmacol. 2007;73:1308–17.
13. Iemura A, Maruiwa M, Yano H, Kojiro M. A new human cholangiocellular carcinoma cell line (KMC-1). J Hepatol. 1992;15: 288–98.
14. Murakami T, Yano H, Maruiwa M, Sugihara S, Kojiro M. Establishment and characterization of a human combined hepatocholangiocarcinoma cell line and its heterologous transplantation in nude mice. Hepatology. 1987;7:551–6.
15. Saito K, Minato H, Kono N, Nakanuma Y, Ishida F, Kosugi M. Establishment of the human cholangiocellular carcinoma cell line (CCKS1). Kanzo. 1993;34:122–9 (in Japanese).
16. Sripa B, Leungwattanawanit S, Nitta T, Wongkham C, Bhudhisawasdi V, Puapairoj A, et al. Establishment and characterization of an opisthorchiasis-associated cholangiocarcinoma cell line (KKU-100). World J Gastroenterol. 2005;11:3392–7.
17. Tepsiri N, Chaturat L, Sripa B, Namwat W, Wongkham S, Bhudhisawasdi V, et al. Drug sensitivity and drug resistance profiles of human intrahepatic cholangiocarcinoma cell lines. World J Gastroenterol. 2005;11:2748–53.
18. Nabekura T, Otsu M, Nagasawa T, Nakauchi H, Onodera M. Potent vaccine therapy with dendritic cells genetically modified by the gene-silencing-resistant retroviral vector GCDNsap. Mol Ther. 2006;13:301–9.
19. Suzuki A, Obi K, Urabe T, Hayakawa H, Yamada M, Kaneko S, et al. Feasibility of ex vivo gene therapy for neurological disorders using the new retroviral vector GCDNsap packaged in the vesicular stomatitis virus G protein. J Neurochem. 2002;82: 953–60.
20. Ishige K, Shoda J, Kawamoto T, Matsuda S, Ueda T, Hyodo I, et al. Potent in vitro and in vivo antitumor activity of interleukin-4-conjugated Pseudomonas exotoxin against human biliary tract carcinoma. Int J Cancer. 2008;123:2915–22.
21. Hirai H, Roussel MF, Kato JY, Ashmun RA, Sherr CJ. Novel INK4 proteins, p19 and p18, are specific inhibitors of the cyclin D-dependent kinases CDK4 and CDK6. Mol Cell Biol. 1995;15: 2672–81.
22. Kato JY, Matsuoka M, Polyak K, Massague J, Sherr CJ. Cyclic AMP-induced G1 phase arrest mediated by an inhibitor (p27Kip1) of cyclin-dependent kinase 4 activation. Cell. 1994; 79:487–96.
23. Blechacz BR, Smoot RL, Bronk SF, Werneburg NW, Sirica AE, Gores GJ. Sorafenib inhibits signal transducer and activator of transcription-3 signaling in cholangiocarcinoma cells by activating the phosphatase shatterproof 2. Hepatology. 2009;50:1861–70.
24. Isomoto H, Kobayashi S, Werneburg NW, Bronk SF, Guicciardi ME, Frank DA, et al. Interleukin 6 upregulates myeloid cell leukemia-1 expression through a STAT3 pathway in cholangiocarcinoma cells. Hepatology. 2005;42:1329–38.
25. Liu L, Cao Y, Chen C, Zhang X, McNabola A, Wilkie D, et al. Sorafenib blocks the RAF/MEK/ERK pathway, inhibits tumor angiogenesis, and induces tumor cell apoptosis in hepatocellular carcinoma model PLC/PRF/5. Cancer Res. 2006;66:11851–8.
26. Yu H, Jove R. The STATs of cancer—new molecular targets come of age. Nat Rev Cancer. 2004;4:97–105.
27. Hirano T, Ishihara K, Hibi M. Roles of STAT3 in mediating the cell growth, differentiation and survival signals relayed through the IL-6 family of cytokine receptors. Oncogene. 2000;19:2548–56.
28. Aggarwal BB, Sethi G, Ahn KS, Sandur SK, Pandey MK, Kunnumakkara AB, et al. Targeting signal-transducer-and-activator-of-transcription-3 for prevention and therapy of cancer: modern target but ancient solution. Ann N Y Acad Sci. 2006;1091: 151–69.
29. Heinrich PC, Behrmann I, Haan S, Hermanns HM, Muller-Newen G, Schaper F. Principles of interleukin (IL)-6-type cytokine signalling and its regulation. Biochem J. 2003;374:1–20.
30. Bollrath J, Phesse TJ, von Burstin VA, Putoczki T, Bennecke M, Bateman T, et al. gp130-mediated Stat3 activation in enterocytes regulates cell survival and cell-cycle progression during colitis-associated tumorigenesis. Cancer Cell. 2009;15:91–102.
31. Grivennikov S, Karin E, Terzic J, Mucida D, Yu GY, Vallabhapurapu S, et al. IL-6 and Stat3 are required for survival of intestinal epithelial cells and development of colitis-associated cancer. Cancer Cell. 2009;15:103–13.
32. Kobayashi S, Werneburg NW, Bronk SF, Kaufmann SH, Gores GJ. Interleukin-6 contributes to Mcl-1 up-regulation and TRAIL resistance via an Akt-signaling pathway in cholangiocarcinoma cells. Gastroenterology. 2005;128:2054–65.
33. Harder J, Riecken B, Kummer O, Lohrmann C, Otto F, Usadel H, et al. Outpatient chemotherapy with gemcitabine and oxaliplatin in patients with biliary tract cancer. Br J Cancer. 2006;95:848–52.
34. Kim ST, Park JO, Lee J, Lee KT, Lee JK, Choi SH, et al. A Phase II study of gemcitabine and cisplatin in advanced biliary tract cancer. Cancer. 2006;106:1339–46.

20132402 8B（別刷 3/6）

厚生労働科学研究費補助金　難治性疾患等克服研究事業

（難治性疾患克服研究事業）

難治性の肝・胆道疾患に関する調査研究

平成23～25年度　総合研究報告書

研究成果の刊行物・別刷（平成24年度）

分冊６－３

研究代表者　坪内　博仁

平成26（2014）年３月

Ⅴ．研究成果の刊行物・別刷
（平成24年度）

分冊６－３

研究成果の刊行に関する一覧表（平成24年度）

書　籍

著者名	論文タイトル名	書籍全体の編集者名	書籍名	出版社名	出版地	出版年	ページ
銭谷幹男	自己免疫性肝炎の診断・治療における最近の知見		最新医学	最新医学社	大阪	2012	27-32
阿部雅則, 恩地森一	原発性胆汁性肝硬変の診断基準と病期分類	田尻久男, 五十嵐正広, 小池和彦, 杉山政則	臨床に役立つ消化器疾患の診断基準・病型分類・重症度の用い方	日本メディカルセンター	東京	2012	187-192
西原利治, 小野正文	非アルコール性脂肪性肝疾患	林紀夫, 日比紀文, 上西紀夫, 下瀬川徹	Annual Review 2012　消化器	中外医学社	東京	2012	139-144
小野正文, 西原利治	NASH/NAFLD の疫学	岡上武	症例に学ぶ NASH/ NAFLD の診断と治療	診断と治療社	東京	2012	2-6
西原利治, 羽柴　基, 小野正文	二次性糖尿病 慢性肝疾患と耐糖能異常		最新臨床糖尿病学	日本臨床社	東京	2012	165-169
西原利治, 小野正文	非アルコール性脂肪肝炎(NASH)の診断基準	田尻久雄, 五十嵐正広, 小池和彦, 杉山政則	臨床に役立つ消化器疾患の診断基準・病型分類・重症度の用い方	日本メディカルセンター	東京	2012	199-203
西原利治, 小野正文	非アルコール性脂肪性肝疾患	跡見裕, 井廻道夫, 北川雄光, 下瀬川徹, 田尻久雄, 渡辺守	消化器疾患診療のすべて	日本医師会	東京	2012	S271-S273
西原利治, 小野正文	脂肪肝	馬場忠雄, 山城雄一郎	新臨床栄養学	医学書院	東京	2012	569-574
西原利治	アルコール性肝障害	山口徹, 北原光夫, 福井次夫	今日の治療指針	医学書院	東京	2012	480-481
藤原慶一, 横須賀收	自己免疫性急性肝不全をどのように診断し治療すべきか	上本伸二	第38回日本急性肝不全研究会記録集　急性肝不全	アークメディア	東京	2013	68-71

井上和明, 渡邊綱正	急性肝炎における EBV と CMV	山本和秀	わが国における急性肝炎の現状　全国調査 2008-2011	中外医学社	東京	2012	46-51
井上和明, 与芝真彰	血漿交換と免疫抑制剤による肝再生の誘導	日本再生医療学会監修/ 後藤一・ 大橋一夫編	再生医療叢書 5 代謝系臓器	朝倉書店	東京	2012	133-140
Inoue K.	Hepatic encephalopathy	Berhardt LV.	Advances in Medicine and Biology	Nova Science Publishers	New York	2012	59-81
大屋敏秀, 田妻　進	胆石症	日本医師会	生涯教育シリーズ-83 消化器疾患診療のすべて	日本医師会雑誌	東京	2012	284-287
菅野啓司, 田妻　進	胆嚢・胆管結石 A 非観血的治療	菅野健太郎	消化器疾患最新の治療 2013-2014	南江堂	東京	2012	385-388
正田純一	漢方薬の有効性と医療科学　インチンコウ湯 漢方薬の薬効と薬理	新井　信, 他	日本伝統医学テキスト　漢方編	厚生労働省	東京	2012	295-297
Shoda J.	Inchinkoto, clinical efficacy and pharmacology	Shin Arai, et al.	Textbook of Traditional Japanese Medicine	厚生労働省	東京	2012	230-232

研究成果の刊行に関する一覧表（平成24年度）

雑　誌

発表者氏名	論文タイトル名	発表誌名	巻号	ページ	出版年
Abe M, Hiasa Y, Onji M.	Dendritic cells in autoimmune liver diseases.	Current Immunology Reviews	8（1）	23-27	2012
阿部雅則，恩地森一	非Ｂ非Ｃ型肝癌 - 最近の知見　AIH における肝癌発生	臨床消化器内科	27（5）	575-579	2012
阿部雅則，恩地森一	消化器疾患診療のすべて　原発性胆汁性肝硬変	日本医師会雑誌	141 特別号（2）	S260-261	2012
Morita S, Joshita S, Umemura T, Katsuyama Y, Kimura T, Komatsu M, Matsumoto A, Yoshizawa K, Kamijo A, Yamamura N, Tanaka E, Ota M.	Association analysis of toll-like receptor 4 polymorphisms in Japanese primary biliary cirrhosis.	Hum Immunol	74	219-222	2013
Nakamura M, Nishida N, Kawashima M, Aiba Y, Tanaka A, Yasunami M, Nakamura H, Komori A, Nakamuta M, Zeniya M, Hashimoto E, Ohira H, Yamamoto K, Onji M, Kaneko S, Honda M, Yamagiwa S, Nakao K, Ichida T, Takikawa H, Seike M, Umemura T, Ueno Y, Sakisaka S, Kikuchi K, Ebinuma H, Yamashiki N, Tamura S, Sugawara Y, Mori A, Yagi S, Shirabe K, Taketomi A, Arai K, Monoe K, Ichikawa T, Taniai M, Miyake Y, Kumagi T, Abe M, Yoshizawa K, Joshita S, Shimoda S, Honda K, Takahashi H, Hirano K, Takeyama Y, Harada K, Migita K, Ito M,	Genome-wide association study identifies TNFSF15 and POU2AF1 as susceptibility loci for primary biliary cirrhosis in the Japanese population.	Am J Hum Genet	91	721-728	2012

Yatsuhashi H, Fukushima N, Ota H, Komatsu T, Saoshiro T, Ishida J, Kouno H, Kouno H, Yagura M, Kobayashi M, Muro T, Masaki N, Hirata K, Watanabe Y, Nakamura Y, Shimada M, HirashimaN, Komeda T, Sugi K, Koga M, Ario K, Takesaki E, Maehara Y, Uemoto S, Kokudo N, Tsubouchi H, Mizokami M, Nakanuma Y, Tokunaga K, Ishibashi H.					
Yoshizawa K, Matsumoto A, Ichijo T, Umemura T, Joshita S, Komatsu M, Tanaka N, Tanaka E, Ota M, Katsuyama Y, Kiyosawa K, Abe M, Onji M.	Long-term outcome of Japanese patients with type 1 autoimmune hepatitis.	Hepatology	56	668-676	2012
銭谷幹男	自己免疫性肝炎の診断・治療における最近の知見	最新医学	67	1811-1816	2012
Oikawa T, Kamiya A, Zeniya M, Chikada H, Hyuck AD, Yamazaki Y, Wauthier E, Tajiri H, Miller LD, Wang XW, Reid LM, Nakauchi H.	SALL4, a stem cell biomarker in liver cancers.	Hepatology	57 (4)	1469-1483	2013
Nakano M, Saeki C, Takahashi H, Homma S, Tajiri H, Zeniya M.	Activated natural killer T cells producing interferon-gamma elicit promoting activity to murine dendritic cell-based autoimmune hepatic inflammation.	Clin Exp Immunol	170	274-282	2012
Hokari A, Ishikawa T, Tajiri H, Matsuda T, Ishii O, Matsumoto N, Okuse C, Takahashi H, Kurihara T, Kawahara K, Maruyama I, Zeniya M.	Efficacy of MK615 for the treatment of patients with liver disorders.	World J Gastroenterol	18	4118-4126	2012
Nakamoto N, Ebinuma H, Kanai T, Chu PS, Ono Y, Mikami Y, Ojiro K, Lipp M, Love PE, Saito H, Hibi T.	CCR9+ Macrophages are Required for Acute Liver Inflammation in Mouse Models of Hepatitis.	Gastroenterology	142	366-376	2012

Yokoo T, Kamimura K, Suda T, Kanefuji T, Oda M, Zhang G, Liu D, Aoyagi Y.	Novel electric power-driven hydrodynamic injection system for gene delivery: safety and efficacy of human factor IX delivery in rats.	Gene Therapy	20 (8)	816-823	2013
Suzuki Y, Ohtake T, Nishiguchi S, Hashimoto E, Aoyagi Y, Onji M,Kohgo Y. The Japan Non-B, Non-C Liver Cirrhosis Study Group.	Survey of non-B, non-C liver cirrhosis inJapan.	Hepatol Res	43 (10)	1020-1031	2013
Takamura M, Yamagiwa S, Matsuda Y, Ichida T, Aoyagi Y.	Involvement of liver-intestine cadherin in cancer progression.	Med Mol Morphol	46 (1)	1-7	2013
Sakamaki A, Kamimura K, Shioji K, Sakurada J, Nakatsue T, Wada Y, Imai M, Mizuno K, Yamamoto T, Takeuchi M, Sato Y, Kobayashi M, Naito M, Narita I, Aoyagi Y.	Immunoglobulin g4-related disease with several inflammatory foci.	Intern Med	52	457-462	2013
Imai M, Higuchi M, Kawamura H, Yoshita M, Takahashi M, Oie M, Matsuki H, Tanaka Y, Aoyagi Y, Fujii M.	Human T cell leukemia virus type 2 (HTLV-2) Tax2 has a dominant activity over HTLV-1 Tax1 to immortalize human CD4(+) Tcells.	Virus Genes	46	39-46	2013
Hara Y, Sato Y, Yamamoto S, Oya H, Igarashi M, Abe S, Kokai H, Miura K, Suda T, NomotoM, Aoyagi Y, Hatakeyama K.	Successful laparoscopic division of a patent ductus venosus: report of a case.	Surg Today	43 (4)	434-438	2012
Kamimura K, Nomoto M, Aoyagi Y.	Hepatic angiomyolipoma: diagnostic findings and management.	Int J Hepatol	2012	410781	2012
Kamimura K, Suda T, Tamura Y, Takamura M, Yokoo T, Igarashi M, Kawai H, Yamagiwa S, Nomoto M, Aoyagi Y.	Phase I study of miriplatin combined with transarterial chemotherapy using CDDP powder in patients with hepatocellular carcinoma.	BMC Gastroenterol	12	127	2012
Oya H, Sato Y, Yamanouchi E, Yamamoto S, Hara Y, Kokai H, Sakamoto T, Miura K, Shioji K, Aoyagi Y, Hatakeyama K.	Magnetic compression anastomosis for bile duct stenosis after donor left hepatectomy: a case report.	Transplant Proc	44	806-809	2012